coefficient, and β is the angle between the local normal and the freestream velocity. From geometric consideration, it is found that

$$\cos^2\beta = \cos^2\alpha \sin^2\theta + \tfrac{1}{2} \sin 2\alpha \sin 2\theta \cos\Phi + \sin^2\alpha \cos^2\theta \cos^2\Phi \quad (4)$$

where α is the angle of attack.

The drag of the body at zero lift can be expressed by substituting Eqs. (3) and (4) into Eq. (1) and imposing $\alpha = 0$, as

$$C_{D_0} = C_{x_{\alpha=0}} = \frac{C_{P_{max}}}{A_r}\int_A \sin^3\theta \, dA \quad (5)$$

We note from geometry that

$$dA = r \, ds \, d\Phi \quad (6)$$

where r is the cylindrical radius and ds is an element of arc length along a body meridian. Substitution into Eq. (5) and integration with respect to Φ yields

$$C_{D_0} = \frac{2\pi C_{P_{max}}}{A_r}\int_0^S \sin^3\theta r ds \quad (7)$$

Considering now the normal-force-curve slope, differentiations of Eq. (2) with respect to the angle of attack α, after substitution of Eq. (3), gives

$$\frac{dC_N}{d\alpha} = C_{N_\alpha} = \frac{C_{P_{max}}}{A_r}\int_A \frac{d(\cos^2\beta)}{d\alpha} \cos\theta \cos\Phi dA \quad (8)$$

and differentiation of Eq. (4) with respect to angle of attack gives

$$[d(\cos^2\beta)/d\alpha] = -2 \sin\alpha \cos\alpha \sin^2\theta + \cos 2\alpha \sin 2\theta \cos\Phi + 2 \sin\alpha \cos\alpha \cos^2\beta \cos^2\Phi \quad (9)$$

which, at $\alpha = 0$, reduces to

$$(d \cos^2\beta/d\alpha)_{\alpha=0} = \sin 2\theta \cos\Phi = 2 \sin\theta \cos\theta \cos\Phi \quad (10)$$

Substituting Eqs. (6) and (10) into Eq. (8) and integrating with respect to Φ results in

$$C_{N_{\alpha_i}} = \frac{2\pi C_{P_{max}}}{A_r}\int_0^S (\sin\theta - \sin^3\theta) r \, ds \quad (11)$$

If we now substitute Eq. (5) and note that $\sin\theta \, ds = dr$, we get

$$C_{N_{\alpha_i}} = (\pi R^2/A_r) C_{P_{max}} - C_{D_0} \quad (12)$$

where R is the maximum cylindrical radius.

In most cases the reference area A_r is equal to πR^2, so that

$$C_{N_{\alpha_i}} = C_{P_{max}} - C_{D_0} \quad (13)$$

Similarly, for the initial-lift-curve slope,

$$C_{L_{\alpha_i}} = C_{P_{max}} - 2C_{D_0} \quad (14)$$

Equations (13) and (14) can be considered as simple rules of thumb for estimating $C_{N_{\alpha_i}}$ or $C_{L_{\alpha_i}}$, because C_{D_0} is usually easier to estimate or calculate. The surprising feature about these relationships is that they are independent of geometry within the limitations of the Newtonian theory for axisymmetric bodies. These relationships are most applicable to noses only because Newtonian theory gives no contribution to $C_{N_{\alpha_i}}$ or $C_{L_{\alpha_i}}$ from cylindrical or convergent afterbodies. However, there is experimental evidence[1] that the derivative of Eq. (14)

$$dC_{L_{\alpha_i}}/dC_{D_0} = -2 \quad (15)$$

is a reasonable rule of thumb, even for noses with cylindrical afterbodies.

The corresponding expressions for $C_{N_{\alpha_i}}$ and $C_{L_{\alpha_i}}$ for symmetric two-dimensional configurations are

$$C_{N_{\alpha_i}} = 2C_{P_{max}}(A_f/A_r) - 2C_{D_0} \quad (16)$$

$$C_{L_{\alpha_i}} = 2C_{P_{max}}(A_f/A_r) - 3C_{D_0} \quad (17)$$

where A_f is the frontal area. The discussion of Eqs. (13) and (14) for axially symmetric flow applies in an analogous fashion to Eqs. (16) and (17).

Reference

[1] Witcofski, R. D. and Woods, W. C., "Static stability characteristics of blunt low-fineness-ratio bodies of revolution at a Mach number of 24.5 in helium," NASA TN D-2282 (1964).

Unsteady Reacting Boundary Layer on a Vaporizing Flat Plate

WARREN C. STRAHLE*
Princeton University, Princeton, N. J.

Nomenclature

B_∞ = $c_p{}^*T_\infty{}^*/\Delta l^*$
c_p = specific heat at constant pressure
D_{12} = binary diffusion coefficient
F = boundary-layer stream-function variable
g = low-frequency expansion functions of P
h = low-frequency expansion coefficients of σ
H, S, V_k, R, U, W_k = high-frequency expansion functions for P, σ, and $\mathcal{Y}_k$
h, s, v_k, r, u, w_k = high-frequency expansion functions for H, S, V_k, R, U, and W_k
i = complex variable $(-1)^{1/2}$
j = stoichiometric mass ratio, oxidizer to fuel
k_k = low-frequency expansion coefficients of $\mathcal{Y}_k$
Δl = latent heat of vaporization
$\mathfrak{L}$ = linear operator
$m = \dfrac{m^*Re^{1/2}}{\rho_\infty{}^*u_\infty{}^*}$ = mass flow rate per unit area
M = Mach number
$\mathfrak{M}$ = space dependent part of m perturbation
$\mathcal{O}[\ ]$ = the order of [ ]
p = pressure
P = space dependent part of ψ perturbation
q = stoichiometric heat of reaction
Re = Reynolds number
$s = L$ = axial distance from leading edge
t = time
T = temperature
u = velocity in s direction
v = velocity in y direction
y = boundary-layer variable in normal direction
Y_k = mass fraction of kth species
$\mathcal{Y}_k$ = space dependent part of Y_k perturbation
α = high-frequency variable
β_1, β_2 = high-frequency boundary-layer variables
γ = ratio of specific heats
ϵ = small perturbation parameter
η = boundary-layer variable
μ = viscosity
$\hat{\mu}$ = boundary-layer variable
ξ = low-frequency boundary-layer variable
ρ = density
σ = space dependent part of T perturbation
τ = liquid temperature

Received February 4, 1965. This work was supported by NASA Grant NsG 99-60.

* Research Associate; now with Propulsion Department, Aerospace Corporation, San Bernardino, Calif. Associate Member AIAA.

ψ = stream function
ω = frequency

Superscripts

$*$ = dimensional quantity
$-$ = steady-state quantity
(i) = ith term of expansion in powers of a parameter or variable

Subscripts

f = flame
F = fuel
k = species k
o = oxidizer
w = wall or liquid surface
∞ = freestream conditions
(i) = ith term in expansion of powers of δM

IN order to gain an idea of the absence of a steady-state pressure gradient, in this note we summarize a treatment of the unsteady flat-plate boundary layer with chemical reaction. This work is a complement to the stagnation-point treatment of a droplet burning in a convective environment with a periodic sound wave imposed upon the freestream.[1] The techniques involved contribute to the general theory of unsteady boundary layers but generalize previous treatments[2,3] to account for compressibility, reaction, a moving boundary (the flame), and to give a treatment uniformly valid in the entire field, free from the blowup at "infinity" noted by Illingworth.[3]

The fundamental assumptions for the flat-plate problem are as follows:

1) The continuum, laminar, unsteady boundary-layer equations hold for conservation of momentum, mass, species, and energy.

2) There is heat transfer by conduction only; no radiation is considered.

3) There are no over-all mass sources, although the flame is a species mass source and sink.

4) Mass diffusion occurs by a mass fraction gradient only. Thermal and pressure diffusion are neglected (see assumption 9).

5) The mixture at any point in the gas is a binary fluid. Only two species are allowed, e.g., fuel vapor and a fictitious single-component product gas.

6) There are no over-all or preferential species body forces.

7) Each component of the gas mixture is thermally and calorically perfect.

8) The viscosity, density-binary diffusion coefficient ($\rho^* D_{12}^*$), and thermal conductivity are proportional to the first power of temperature.

9) The specific heats of each species are the same implying equal molecular weights and justifying the fourth assumption.

10) Reaction is instantaneous and complete, implying a collapsed, zero thickness flame with a stoichiometric consumption rate at the flame.

11) There is zero tangential slip velocity at the liquid-gas surface, and the liquid is stationary (infinite liquid viscosity).

12) The liquid-gas interface is in equilibrium implying infinitely fast evaporation kinetics.

13) The liquid density is very large compared to the gas such that the normal gas velocity at the interface is much larger than the liquid regression velocity.

14) The liquid is at its wet bulb temperature so that all heat transfer at the interface goes toward liquid vaporization, not transient temperature change. This is assumed also in the unsteady state. A variable mass fraction of liquid vapor at the interface is, however, allowed.

15) The Mach number is small such that $M^2 \ll 1$.

The validity of these assumptions is discussed at length by Strahle.[4] The unsteadiness is introduced by assuming a small amplitude, isentropic, traveling sound wave in the freestream parallel to the flat plate of the form

$$\left.\begin{aligned} u(s, y = \infty) &= 1 + \epsilon e^{i\omega(t+\delta Ms)} + \mathcal{O}[\epsilon M^2] + \mathcal{O}[\epsilon^2] \\ \gamma M^2 p(s, \infty) &= 1 - \epsilon\gamma\delta M e^{i\omega(t+\delta Ms)} \\ T(s, \infty) &= 1 - \epsilon\delta M(\gamma - 1) e^{i\omega(t+\delta Ms)} \\ Y_o(s, \infty) &= \bar{Y}_{o_\infty} \end{aligned}\right\} \quad (1)$$

where u is parallel velocity nondimensionalized by the freestream u_∞^*, p is pressure nondimensionalized by the dynamic head $\rho_\infty^* u_\infty^{*2}$, T is temperature made dimensionless by the freestream temperature T_∞^*, and Y_o is the oxidizer mass fraction. ϵ is a small parameter very much less than unity; ω is the frequency made dimensionless by L^*/u_∞^*, L^* being a characteristic length from the leading edge; t is time made dimensionless by L^*/u_∞^*; and s is the distance from the leading edge nondimensionalized by L^*. Since in the flat plate there is in reality no characteristic length, $L^* = s^*$ and $s = 1$. $\delta = \pm 1$ depending on whether the wave is traveling left or right.

Under a Howarth-Moore unsteady transform

$$\hat{\mu} = \int_0^y \rho(x, y, t)dy \qquad x = s \qquad t = t$$
$$\eta = \hat{\mu}/2x^{1/2} \qquad u = \psi_{\hat{\mu}} \qquad v = -(1/\rho)(\psi_s + \hat{\mu}_t) \quad (2)$$

and the assumption of the solution in the form

$$\left.\begin{aligned} \psi &= 2x^{1/2}[F(\eta) + \epsilon P(\eta, x) e^{i\omega(t+\delta Ms)}] \\ T &= \bar{T}(\eta) + \epsilon\sigma(\eta, x) e^{i\omega(t+\delta Ms)} \\ Y_k &= \bar{Y}_k(\eta) + \epsilon\mathcal{Y}_k(\eta, x) e^{i\omega(t+\delta Ms)} \end{aligned}\right\} \quad (3)$$

the steady state consists of the usual Blasius equation and well-known mass and energy transport equations. These are solved elsewhere and are a well-known solution of the steady-state boundary layer.[4,5] The interest here is in the first-order perturbation set, obtainable by a substitution of Eqs. (3) into the boundary-layer equations and collecting the coefficients of the first power in ϵ. These are

$$P_{\eta\eta\eta} + FP_{\eta\eta} + F''P - 2\xi[F'P_{\eta\xi} - F''P_\xi] - 2\xi[F'P_\eta - F''P]\delta M - 2\xi P_\eta = -2\xi(1 + \delta M)\bar{T} + \gamma\delta MF''' \quad (4a)$$

$$\mathfrak{L}[\sigma] = \left[\frac{\partial^2}{\partial\eta^2} + F\frac{\partial}{\partial\eta} - 2\xi F'\frac{\partial}{\partial\xi} - 2\xi(1 + \delta MF')\right]\sigma = -P\bar{T}'(1 + 2\xi\delta M) - 2\xi P_\xi\bar{T}' + \gamma\delta M\bar{T}'' + 2\xi\delta M(\gamma - 1)\bar{T} \quad (4b)$$

$$\mathfrak{L}[\mathcal{Y}_k] = -P\bar{Y}_k'(1 + 2\xi\delta M) - 2\xi P_\xi\bar{Y}_k' + \gamma\delta M\bar{Y}_k'' \quad (4c)$$

which are unlike the stagnation-point problem[1] since they are partial differential equations. They are subject to boundary conditions at the surface, flame, and freestream implied previously and fully developed in Ref. 4. The flame boundary is most troublesome since it moves in time under the soundwave action. No method of solution has been found for the full-frequency range, so resort is made to two regions, low-and high-frequency.

For the low-frequency case, an expansion is assumed of the form

$$\left.\begin{aligned} P &= \sum_{n=0}^{\infty} (2\xi)^n g^{(n)}(\eta) \\ \sigma &= \sum_{n=0}^{\infty} (2\xi)^n h^{(n)}(\eta) \\ \mathcal{Y}_k &= \sum_{n=0}^{\infty} (2\xi)^n k_k^{(n)}(\eta) \end{aligned}\right\} \quad (5)$$

convergence of which for some neighborhood of ξ about zero is suggested by Ref. 2 but is not claimed here. Then to make computations independent of δM, a further expansion is assumed of the form $g^{(n)} = g_{(0)}{}^{(n)} + \delta M g_{(1)}{}^{(n)}$ and similarly for the other variables. This latter manipulation is not without physical significance, as explained in Ref. 4. This expansion produces a doubly infinite set of equations for each of P, σ, and $\mathcal{Y}_k$. The $\binom{0}{0}$, $\binom{1}{0}$, and $\binom{0}{1}$ cases have been numerically integrated and are located in Ref. 4. The fundamental conclusion drawn is that qualitatively (although, of course, numerically different) the results are similar to those of the stagnation point.[1, 4] The primary quantities of interest, the wall vaporization rate $\mathfrak{M}_w$ and the flame burning rate $\mathfrak{M}_{F_f}$ given by

$$2x^{1/2}m_w = 2x^{1/2}\overline{m}_w + \epsilon\mathfrak{M}_w\, 2x^{1/2}e^{i\omega(t+\delta Mx)}$$

$$2x^{1/2}m_{F_f} = 2x^{1/2}\overline{m}_{F_f} + \epsilon\mathfrak{M}_{F_f}2x^{1/2}e^{i\omega(t+\delta Mx)}$$

behave as with the stagnation point with parameter changes.

The high-frequency ($\xi \gg 1$) results are extracted by introducing the high-frequency variable $\alpha = \xi^{-1/2}$. Use of this variable in Eqs. (4) yields the following set of equations:

$$P_\eta + \delta M[F'P_\eta - F''P] = (1 + \delta M)\bar{T} + (\alpha^2/2)[P_{\eta\eta\eta} + FP_{\eta\eta} + F''P - \gamma\delta MF'''] + (\alpha^3/2)[P_{\eta\alpha}F' - P_\alpha F''] \quad (6a)$$

$$(1 + \delta MF')\sigma = \delta MP\bar{T}' - \delta M(\gamma - 1)\bar{T} + (\alpha^2/2)[\sigma_{\eta\eta} + F\sigma_\eta + P\bar{T}' - \gamma\delta M\bar{T}''] + (\alpha^3/2)[\sigma_\alpha F' - \bar{T}'P_\alpha] \quad (6b)$$

$$(1 + \delta MF')\mathcal{Y}_k = \delta MP\bar{Y}_k' + (\alpha^2/2)[\mathcal{Y}_{k\eta\eta} + F\mathcal{Y}_{k\eta} + P\bar{Y}_k' - \gamma\delta M\bar{Y}_k''] + (\alpha^3/2)[\mathcal{Y}_{k\alpha}F' - \bar{Y}_k'P_\eta] \quad (6c)$$

Then with $\beta_1 = 2^{1/2}\eta/\alpha$ and $\beta_2 = (2^{1/2}/\alpha)(\eta - \bar{\eta}_f)$ a solution of Eqs. (6) is sought of the form

$$P = H(\alpha, \eta) + R_1(\alpha, \beta_1) + R_2(\alpha, \beta_2)$$

$$\sigma = S(\alpha, \eta) + U_1(\alpha, \beta_1) + U_2(\alpha, \beta_2)$$

$$\mathcal{Y}_k = V_k(\alpha, \eta) + W_{k1}(\alpha, \beta_1) + W_{k2}(\alpha, \beta_2)$$

on each side of the flame. The subscript 1 parts do not exist on the freestream side of the flame, only on the liquid side. Because of the linearity of the problem, these functions may be and are picked in the following manner: the H, S, and V parts satisfy the full Eqs. (6), whereas the R, U, and W parts only satisfy the homogeneous parts. The R, U, and W parts bring back the highest derivatives in Eqs. (6) in the limit as $\alpha \to 0$ since $\partial/\partial\eta = (1/\alpha)(\partial/\partial\beta)$. This is necessary to satisfy all the boundary conditions. The subscript 1 solutions are important near the wall, and subscript 2 are important near the flame; each may be picked to have exponential decay away from their respective boundaries. These form localized "high-frequency boundary layers" near the flame and wall and occur because the cycle times have become too short compared to diffusion times for the diffusion processes to keep up with the oscillating field and to smooth out the field. Away from these boundaries, where the diffusion processes are generated, the H, S, and V solutions hold in the majority of the field.

To complete the solution, we assume regular expansions of the form

$$H = \sum_{n=0}^{\infty} \alpha^n h^{(n)}(\eta) \qquad R = \sum_n \alpha^n r^{(n)}(\beta)$$

$$S = \sum_n \alpha^{(n)} s^{(w)}(\eta) \qquad U = \sum_n \alpha^n u^{(n)}(\beta)$$

$$V_k = \sum_n \alpha^n v_k{}^{(n)}(\eta) \qquad W_k = \sum_n \alpha^n w_k{}^{(n)}(\beta)$$

which results in a series of ordinary differential equations in η as the independent variable. Upon similar expansion of the boundary conditions and of F as

$$F = \sum_{n=0}^{\infty} a_{w_n}(\alpha\beta_1)^n$$

near the wall and as

$$F = \sum_{n=0}^{\infty} a_{f_n}(\alpha\beta_2)^n$$

near the flame, it may be shown[4] that a recursive procedure will determine all the unknown functions. Then computation of $\mathfrak{M}_w$ and $\mathfrak{M}_{F_f}$ yields

$$\frac{\mathfrak{M}_w}{\overline{m}_w} = \frac{2^{1/2}\delta M\bar{B}_\infty\bar{\tau}(\gamma - 1)}{F(0)}\left(\frac{1}{\alpha}\right) + \mathcal{O}[1] \quad (7)$$

$$\frac{\mathfrak{M}_{F_f}}{m_{F_f}} = -\delta M[(\gamma - \bar{T}_f) + m_{F_f}q\alpha + \mathcal{O}(\alpha^2)] \quad (8)$$

Concerning Eq. (7), the vaporization rate perturbation goes to infinity as $i\omega x^{1/2}$. This may have been suspected since heat transfer at the wall behaves in the same manner.[3] The reason again lies in the fact that diffusion is too slow. Compression heating raises the gas temperature near the wall isentropically [note the $\gamma - 1$ factor in Eq. (7)] before the diffusion can smooth out the field. Since the liquid temperature is constant, a very strong temperature gradient appears near the wall, causing high heat transfer and, hence, vaporization. Note, as expected from the discussion, that to $\mathcal{O}[1]$ this result requires fluid compressibility ($M > 0$) and that, because of the appearance of δ, this will follow the pressure (or any other state variable) perturbation regardless of the wave form built by superposition. Superposition is valid because of the linearity of the problem. This corresponds to the $\binom{n}{1}$ portions of the low-frequency solution previously mentioned.

Considering the burning-rate perturbation, it is bounded in the limit as $\alpha \to 0$. This occurs since the flame can move and destroy any strong gradients in its vicinity. This result to $\mathcal{O}[\alpha^2]$ also requires fluid compressibility and will follow the pressure perturbation. It is identical in form (but not numerically) to the stagnation-point treatment[1, 4] as is the vaporization rate behavior. For $T_f > \gamma$, the burning rate is negative with respect to the pressure as $\alpha \to 0$, but it approaches this limit from the side in phase with the pressure, since $m_{F_f}q$ is always positive and $\alpha = e^{-i\pi/4}/\omega x^{1/2}$.

Although this procedure may be carried to higher orders in α, the algebraic complexity begins to mount rapidly. The high-frequency solution should also not be construed as a convergent procedure. It is at best only an asymptotic representation.

On a qualitative basis, since both the low-frequency and high-frequency results are similar to those of the stagnation point, it appears reasonable to use those of the stagnation-point treatment; for that problem an exact solution is known over the full-frequency range. The problem here, of course, is that the intermediate frequency transition from the low- to high-frequency results is not known for the flat plate and may vary markedly from the stagnation-point behavior. The only possibility to resolve this difficulty is to work out more terms of the low- and high-frequency expansions. This has not yet been done.

References

[1] Strahle, W. C., "Periodic solutions to a convective droplet burning problem," Proc. 10th Intern. Symp. Combust. (to be published).

[2] Lam, S. H. and Rott, N., "Theory of linearized time-dependent boundary layers," Cornell University, Air Force Office of Scientific Research TN-60-1100 (July 1960).

[3] Illingworth, C. R., "The effects of a sound wave on the compressible boundary layer on a flat plate," J. Fluid Mech. **3**, 471–479 (1958).

[4] Strahle, W. C., "A theoretical study of unsteady droplet burning: Transients and periodic solutions," Princeton Univ. Aeronautical Engineering Lab. Rept. 671 (1963).

[5] Schlichting, H. and Bussmann, K., "Exakte Lösungen für die laminare Grenzschict mit Absaugung und Ausblasen," Schriften Deutscher Akad. Luftfahrtforshung **7**, 25–35 (1953).

Electrode Drops and Current Distributions in an MGD Channel

JOHN J. KARKOSAK*
United Aircraft, Inc., East Hartford, Conn.
AND
MYRON A. HOFFMAN†
Massachusetts Institute of Technology, Cambridge, Mass.

Introduction

THE performance of electrodes in MGD channel flows is of importance in both MGD generator and accelerator applications. It has been predicted by Kerrebrock[1] that large boundary-layer drops may result from a cold electrode wall for the case of equilibrium electrical conductivity. In addition, Podolsky and Sherman[2] and Hurwitz, Kilb, and Sutton[3] have predicted large current concentrations at the corners of both continuous and segmented electrodes. Since these phenomena would seriously limit the performance of MGD generators and accelerators, an experimental investigation is in progress to evaluate their importance. This technical note summarizes the initial results on a continuous electrode geometry.[4]

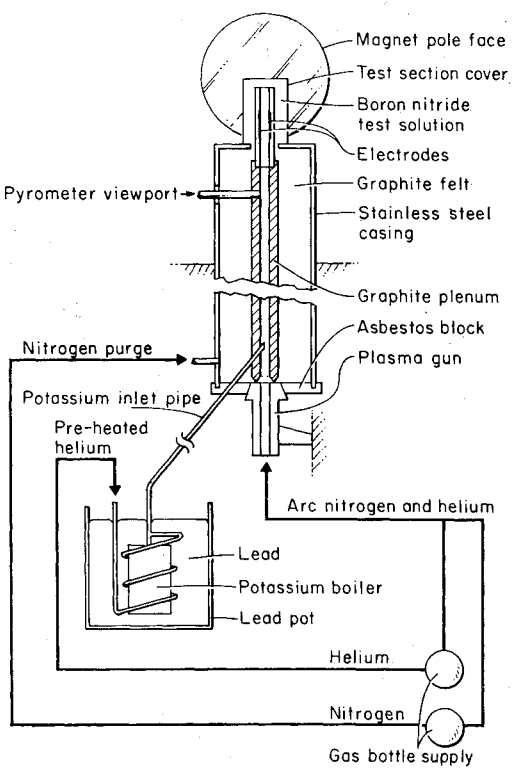

Fig. 1 Schematic diagram of test facility.

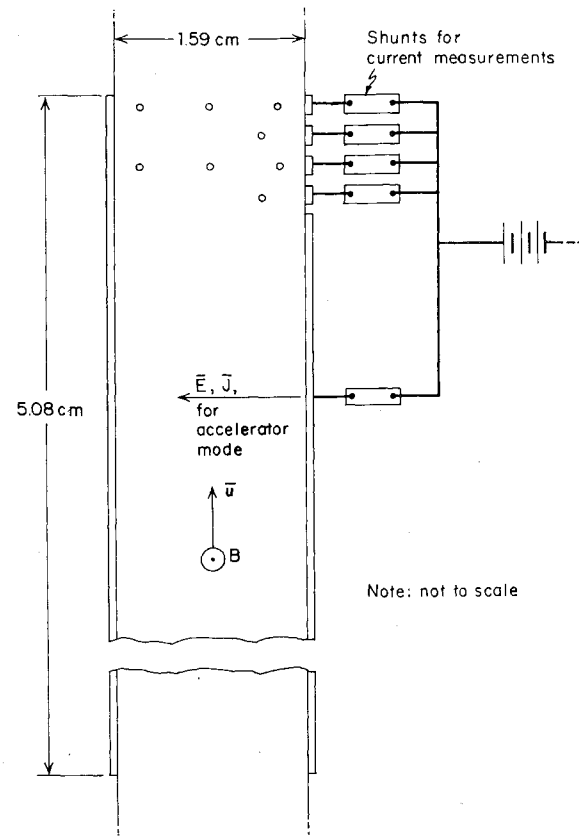

Fig. 2 Schematic diagram of the test section and current measurement circuit.

Experimental Facility and Operating Conditions

The experimental facility shown in Fig. 1 consists of an arc heater and graphite plenum surmounted by a boron nitride test section. The test gas is primarily helium mixed with a nitrogen mole fraction of about 11% to obtain higher gas temperatures. A part of the gas is preheated in a pot of molten lead to about 1000°K. A stainless-steel boiler filled with potassium is immersed in the lead pot and injects approximately 0.3% potassium into the preheated gas stream through a choked orifice. The arc flow and the seeded flow mix in a graphite plenum and then are passed through the test section.

For the tests to be described, the total gas pressure was approximately 1 atm, and the gas temperature as measured by a pyrometer was about 1680°K. The average electrode temperature was found to be 1350°K using a platinum − platinum + 10% rhodium thermocouple attached to the rear of one electrode. The flow velocity calculated from measured flow rates and the gas temperature is estimated to have been about 100 m/sec in the test section.

The test section shown in Fig. 2 has a square cross section of 1.59 cm on a side. It is made of boron nitride and contains one pair of tantalum electrodes with a length to channel height ratio of 3.2. The exit end of one of the electrodes has been subdivided into four small pieces and one large piece, which are electrically insulated from each other by thin boron nitride spacers in the channel wall. However, they are all electrically connected to each other externally after the current-measuring shunts. Using this simple technique, it has been possible to obtain a measure of the current distribu-

Received February 15, 1965. This work was carried out under NASA Grant No. 496 through the Massachusetts Institute of Technology, Center for Space Research.

* Engineer, Advanced Power Systems Group. Student Member AIAA.

† Associate Professor, Department of Aeronautics and Astronautics. Member AIAA.